JOURNAL OF GEOPHYSICAL RESEARCH, VOL. 112, D11103, doi:10.1029/2006JD007291, 2007

Decadal changes in 1870–2004 Northern Hemisphere winter sea level pressure variability and its relationship with surface temperature

M. R. Haylock,[1] P. D. Jones,[1] R. J. Allan,[2] and T. J. Ansell[2]

Received 10 March 2006; revised 19 October 2006; accepted 14 January 2007; published 1 June 2007.

[1] Decadal changes in correlations between boreal winter averages of indices of the North Atlantic Oscillation (NAO) and average temperature north of 20°N (NH20N) have been reported in the literature. We show that such fluctuations are caused by changing midfrequency and high-frequency correlations (periods less than 30 years) and are not the result of changes in the station network or a few erratic years. By examining the NAO-temperature squared correlation on a spatial basis, we show that there have been strong decadal changes in the Pacific but a more constant relationship in the Atlantic. We explain the varying NAO-temperature relationship by showing that sea level pressure (SLP) variance has changed markedly through time, especially in the North Pacific. We performed a principal component analysis (PCA) of the running variance of SLP using a recently released historical global gridded data set. The first PC corresponded to a reduction in variance of the NAO during the mid-20th century, which occurred concurrently with a similar change in the variance of the El Niño–Southern Oscillation (ENSO). The loading patterns for this PC suggest that the decadal changes in the variability of ENSO could be responsible for the changes in NAO variance. The second North Pacific–dominated PC was indicative of increased variability of the strength of the Aleutian Low during the mid-20th century, during which time the variability in the Pacific and Atlantic were in phase. These two changes in variance of SLP, together with the phase relationship between the two ocean basins, explain the changing NAO-temperature correlation.

Citation: Haylock, M. R., P. D. Jones, R. J. Allan, and T. J. Ansell (2007), Decadal changes in 1870–2004 Northern Hemisphere winter sea level pressure variability and its relationship with surface temperature, *J. Geophys. Res.*, *112*, D11103, doi:10.1029/2006JD007291.

1. Introduction

[2] Winter sea level pressure (SLP) in the Northern Hemisphere (NH) exhibits its largest interannual variability through the North Atlantic Oscillation (NAO) [*Hurrell et al.*, 2003]. The term NAO was first used by *Walker* [1924] to describe the out-of-phase behavior of monthly averaged sea level pressure between Iceland and the Azores. Its importance in modulating European climate is evident in the abundance of studies linking the NAO to a multitude of responses, for example European temperature and precipitation [*Trigo et al.*, 2002], sea level in the Baltic [*Yan et al.*, 2004], Eurasian snow cover [*Saito et al.*, 2004], ice conditions in the Baltic Sea [*Jevrejeva et al.*, 2003], streamflow in the Middle East [*Cullen et al.*, 2002] and the chemistry and ecology of lakes in northern England [*George et al.*, 2004]. The influence of the NAO extends to other parts of the NH. During the positive index phase in the western Atlantic, anomalous cold northerly flow occurs over Greenland and northeast Canada associated with anticlockwise circulation about the Iceland low. Similarly warm conditions in the southeast United States result from clockwise circulation about the Atlantic subtropical high [*Hurrell et al.*, 2003].

[3] Most of the studies examining NAO teleconnections have assumed a stationary relationship. However, a few studies have indicated that the strength of NAO-climate relationship changes with time [*Jones et al.*, 2003; *Osborn et al.*, 1999; *Raible et al.*, 2001; *Slonosky et al.*, 2001; *Walter and Graf*, 2002]. In particular, *Jones et al.* [2003] used 31-year running correlations of three December-March (DJFM) NAO indices with a variety of NH climate indices to show how correlations have varied over time. They concluded that correlations between the Gibraltar-Reykjavik DJFM NAO index [*Jones et al.*, 1997] and DJFM land temperature averaged across stations north of 20°N [*Jones et al.*, 1999] were much lower in the period 1935–1955 than in the late 19th and late 20th centuries. In contrast, the correlation with temperature averaged across northern and central Europe (40–70°N, 10°W–30°E) has remained relatively constant.

[4] Further analyses of the nonstationary NAO-temperature relationship are provided by *Raible et al.* [2001] and *Walter*

[1]Climatic Research Unit, School of Environmental Sciences, University of East Anglia, Norwich, UK.
[2]Hadley Centre for Climate Prediction and Research, Met Office, Bracknell, UK.

and Graf [2002], who examined the changing correlations between the NAO and sea surface temperatures (SST) in observational data [*Walter and Graf*, 2002] and a 600 year coupled global climate model (GCM) experiment [*Raible et al.*, 2001]. Both studies concluded that periods with strong correlations between the NAO and North Atlantic SST coincided with strong decadal variability in the NAO. Periods when the correlation was low also saw low NAO decadal variability and, importantly, a strong Pacific–North American (PNA) pattern linking the Pacific and North Atlantic regions.

[5] The main aim of this study is to examine the changing NAO-temperature relationship in more detail. It is important to document the degree of stationarity in these relationships, because in many applications stationarity is assumed. Statistical downscaling is one area where stationarity of statistical relationships is crucial. Although the NAO is an important signal in explaining the large-scale changes in extreme winter rainfall over recent decades [*Haylock and Goodess*, 2004], stationarity concerns may limit its usefulness as a predictor when used to downscale climate models to determine possible changes in extreme rainfall in the future.

[6] Stationarity is also an important issue for the proxy reconstruction of the NAO index. *Cook* [2003] suggests the changing NAO teleconnections as a possible reason why previous proxy NAO reconstructions validated poorly when calibrated and validated over different periods of the instrumental record.

[7] Of more practical significance is the use of NAO teleconnections for seasonal forecasting. NAO relationships with Atlantic SST and European climate [*Rodwell et al.*, 1999] have been used by the UK Met Office to issue experimental seasonal forecasts for winter temperature and precipitation. The forecast methodology involved a maximum covariance analysis between May SST and the following winter 500 hPa geopotential height, from which the expected magnitude of the NAO can be derived. The forecasted NAO value was then used to qualitatively determine expected temperature and precipitation over Europe on the basis of historical (assumed stationary) relationships.

[8] Of no less significance is the examination of changing NAO teleconnections in order to extend our understanding of important processes in the climate system. Many of the studies referenced above examine only the later decades of the 20th century. This limitation arises because of either the limits of the data that are being linked to circulation changes or the dependence on NCEP/NCAR reanalyses for circulation data. In this study we use long-term data sets for NAO indices, gridded temperature, and newly gridded pressure data. The emphasis is on long records to show that examining links using just the recent decades may not be representative of what has happened in earlier decades and therefore not what may occur in the future.

[9] The first task of this study is to examine in more detail the changing NAO-temperature relationship (section 2). Here we construct our own index of average NH temperature north of 20°N (NH20N) based on a fixed selection of gridded land and sea observations to ensure consistent geographical coverage for the analysis period. We also test whether a few extreme years are affecting the running correlations and whether the changing correlations are due to changing low frequencies, such as strong warming trends in the most recent decades. In section 2 we also argue that by including regions that are both positively and negatively correlated with the NAO, it is more prudent to examine the squared correlations between each grid point and the NAO averaged across the NH rather than the correlation between the average NH temperature and the NAO. We expect this would give a better measure of the changing strength of the NAO-temperature relationship, independent of the changing sign of the relationship at each location.

[10] Section 3 examines the cause of the changing NAO-NH20N correlations. We can rule out global warming as a possible cause of the changing correlations as the running correlations, with their equivalent highs in the late 19th and 20th centuries share no similarity to the warming trend (as shown by *Folland et al.* [2001, Figure 2.7]).We first show that correlations of NH20N with the SOI and several NH circulation indices are much lower than with the NAO, and NH20N is best modeled using just the NAO and an index of pressure in the North Pacific. In seeking a cause for the changing pressure-temperature relationship, we build on the work of previous studies which indicate that the variance of the NAO has changed through time [*Feldstein*, 2002; *Raible et al.*, 2001; *Walter and Graf*, 2002]. We also examine the changing NAO-temperature relationship, by seeking to isolate the evolving spatial pattern of NH SLP variability. By showing how the magnitude of interannual variability of SLP changes with time and space, we provide an insight into the changing nature of correlations between temperature and indices of SLP such as the NAO. Our examination of the link between changing correlations and changing SLP variance is key to this study and is based on the simple premise that, with less active SLP variability, one might expect less active teleconnections. This hypothesis is supported by the close statistical relationship between correlation and covariance. We show that SLP variance has indeed changed markedly through time, especially in the North Pacific. Importantly, in support of our variance-teleconnection hypothesis, we demonstrate that the changing NH total SLP variance accounts for about 40% of the changing NAO-temperature relationship. Finally, section 4 discusses the implications of this study, particularly with regard to the influence of the El Niño–Southern Oscillation (ENSO) phenomenon on the NAO-NH20N relationship.

2. Correlation Between Northern Hemisphere Temperature and the NAO

[11] The 1870–2004 HadCRUT2v land-sea temperature anomaly data set forms the basis for this part of the study. This monthly $5 \times 5°$ gridded data set combines over 3000 land stations [*Jones and Moberg*, 2003] with SST taken from ship observations. The variance of each grid point is adjusted to take into account the changing number of observations that constitute each grid box average [*Jones et al.*, 2001].

[12] The time series of the average land temperature anomaly north of 20°N used in the analysis of *Jones et al.* [2003] is constructed using a changing station network. We need to eliminate potential variability related to the changing station network from the analysis to be certain that

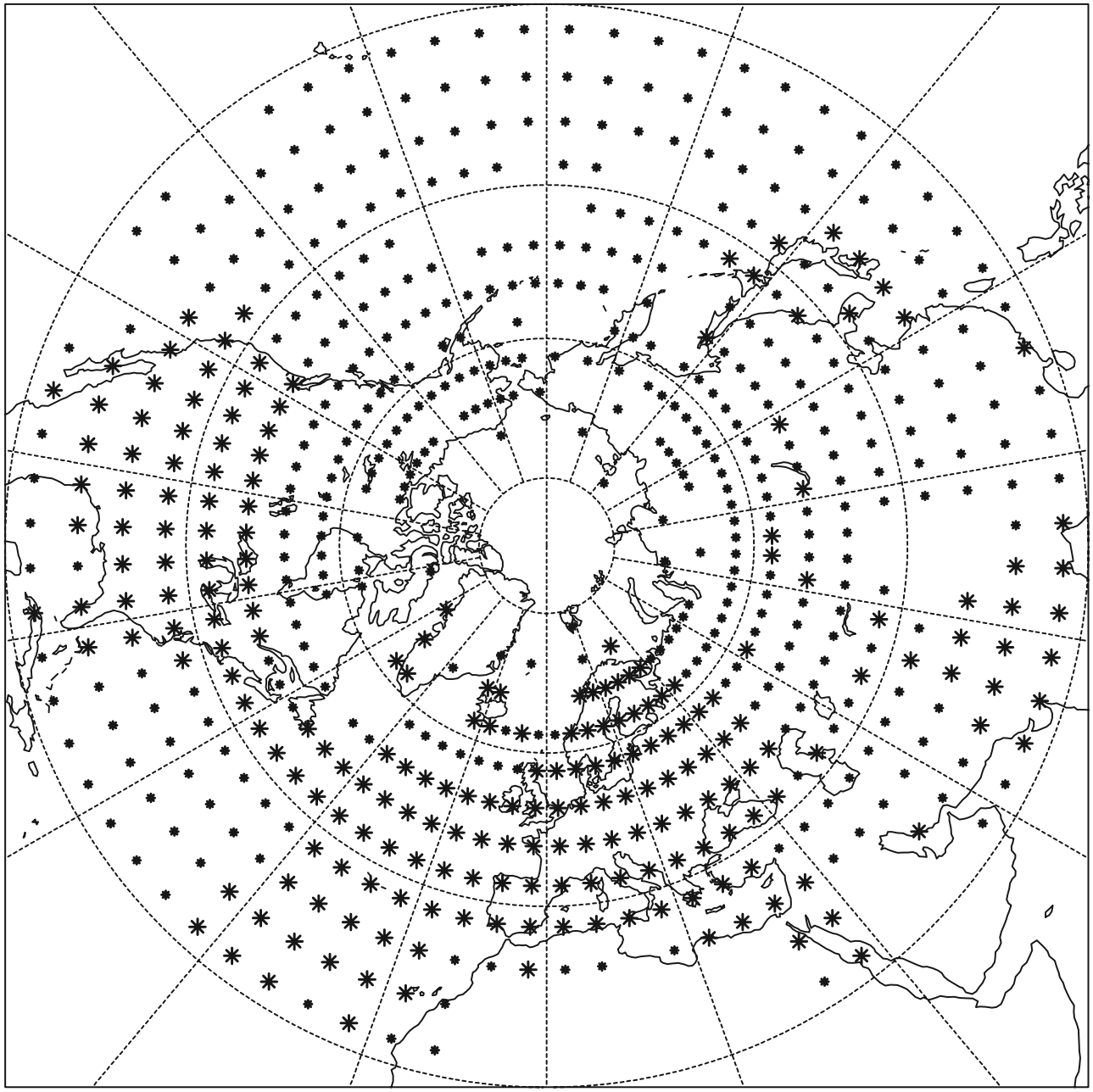

Figure 1. Location of HadCRUT2v grid points used in the study. Small points are only in the 1926–2004 data set. Larger points are used for the 1870–2004 and 1926–2004 studies.

the changing NAO-temperature correlation is not just due to a greater number of poorly correlated station data in the middle of the 20th century, although this is highly unlikely given the steady increase in geographical coverage of the network. The coverage of the HadCRUT2v data set changes with time as there is no interpolation of data to grid boxes lacking observations. Therefore we selected from the data set those grid points north of 20°N that have at least 21 nonmissing DJFM averages in any 31-year period for 1870–2004, where a DJFM average is only calculated if there are at least three of the four months present. The location of these 224 points is shown by the large points in Figure 1. Coverage is poor over the Pacific, West Atlantic, Africa, the Middle East and Eastern Asia. North of 60°N, the coverage is concentrated in the European sector. To increase the coverage significantly we need to greatly shorten the period. We have therefore included a more spatially complete set based on the period 1926–2004 which has 614 points, also shown in Figure 1. This period was chosen as the period that maximizes the product of the period length and the number of grid points selected using the above criteria. All points in the longer period set are present in the shorter period set.

[13] Figure 2 is a repeat of the analysis of *Jones et al.* [2003] but using a latitude-weighted average of the grid points in Figure 1 to create the mean NH DJFM temperature north of 20°N (NH20N) according to equation (1). Note

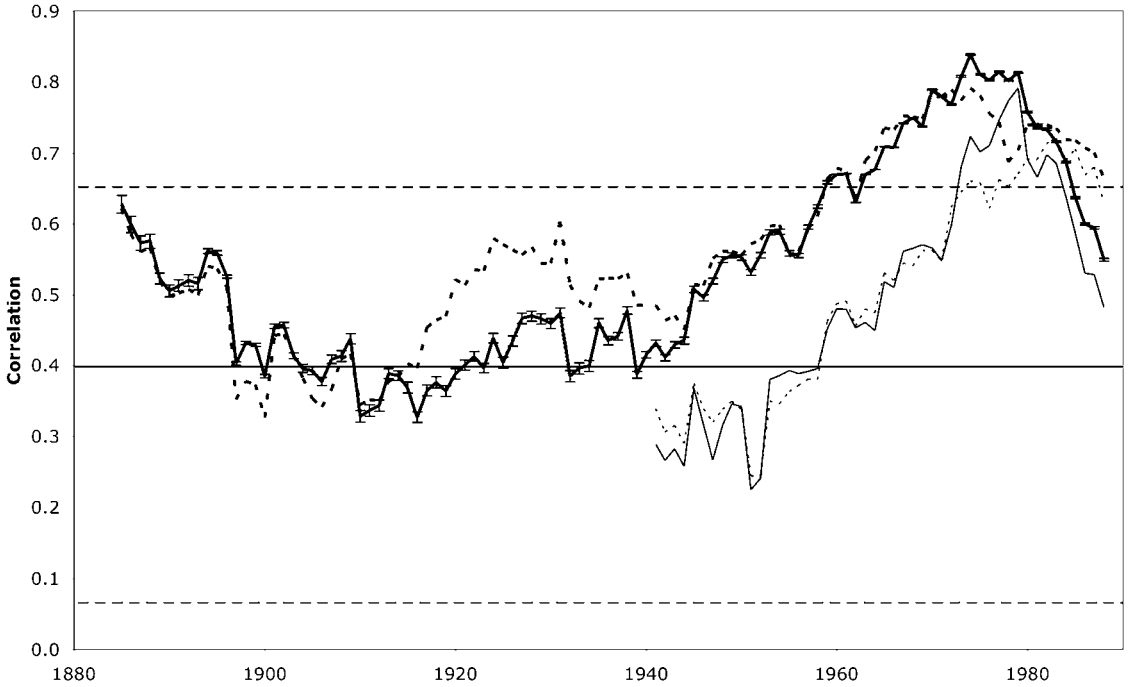

Figure 2. DJFM 31-year running correlation between the NAO index and average NH land and sea temperature north of 20°N (thick solid line) and using high-pass filtered data (thick dashed line) and using the shorter data set for unfiltered (thin solid line) and high-passed (thin dashed line) data. Horizontal lines show the median (solid) and 2.5% and 97.5% (dashed) confidence limits for 31-year correlations sampled from a first-order regression process (see text). Error bars on the unfiltered longer series (thick solid line) arise from missing data (see text).

that, whereas *Jones et al.* [2003] used land points only, Figure 2 incorporates marine data.

$$NH20N_t = \frac{\sum \cos(lat) T_t}{\sum \cos(lat)} \quad (1)$$

[14] Figure 2 includes error bars on the running correlation related to the influence of missing data. To calculate the error bars, we filled missing monthly mean temperature values at each grid point by assuming a first-order autoregressive process. We did this 10,000 times with differing random high-frequency error, but maintaining the long-term first-order autocorrelation in the monthly series. In each realization we gap filled the monthly temperature data at each grid point, calculated the DJFM NH20N index, then calculated the running correlation with the NAO. From the 10,000 samples we calculated the 2.5% and 97.5% confidence limits. These limits are very small (<0.02) compared with the decadal variability in the correlation (>0.3). Therefore the secular change in the correlation cannot be explained by a change in the amount of missing data through time.

[15] Figure 2 also gives the median and 2.5% and 97.5% confidence limits for running 31-year correlations between two random normally distributed series with the same long-term correlation as the NAO and NH20N (0.39) as determined by a Monte Carlo simulation. In this experiment we generated 10,000 pairs of 31-point series using a first-order regression process and calculated their correlation. The confidence limits show that while the changes up until 1960 are within what would be expected by random sampling of two long series with a stationary correlation, the large positive correlations since 1960 are unusual ($p < 0.05$).

[16] Figure 2 reveals a similar change in the NAO-NH20N correlation to what was found by *Jones et al.* [2003], from an initial high of 0.63 in 1885 to a low of 0.33 in 1916 then increasing to a high of 0.84 in 1974 and declining in later years. Although the general shape of the series is the same in Figure 2 and the earlier study, the year with the lowest correlation appears earlier in our analysis. Throughout this study, where we refer to 31-year running windows, we indicate time by referring to the central year (e.g., 1989 for the period 1974–2004). The high correlations reached in the later decades of the analysis are likely to be enhanced by the strong positive trends in both the NAO and NH20N in this period. Since we are primarily interested in correlations of interannual variability of the NAO and NH20N, we have removed the low frequencies with periods greater than 30 years from the two series before calculating running correlations. The low-frequency temperature signal shows strong warming in two periods (1910–1940 and 1970–present) while the NAO shows a general decline from 1910 to 1960 followed by a rising trend (as shown by *Folland et al.* [2001, Figures 2.7 and 2.30]). Repeating the running correlations between the NAO and NH20N with the high-pass filtered data gives the thick dashed line in Figure 2. This enhances the minor peak in 1931 and reduces slightly the highs reached in the later years (0.80 compared with 0.84 in 1974). The lowest correlation of the filtered data is 0.33 in 1900. There are, nevertheless, marked

changes in correlations between the high-frequency components of the data. Therefore the change in correlations through the 20th century is not due to changes in the relative phases of the low frequencies of the two series but primarily due to the changing correlation of frequencies with periods less than 30 years. We can also conclude that the change in correlations is not due to a change in the HadCRUT2v spatial coverage, as this was kept constant for this analysis, unlike the temperature series used by *Jones et al.* [2003], which was based on a changing station network.

[17] We repeated the running correlation using the shorter, more spatially complete data set, as shown in Figure 2. This gives rise to a similar strong increase in the later part of the record but starting from an initial low of 0.23 in 1951 and reaching a high of 0.79 in 1979. This change in correlation in the later decades using the shorter set is more pronounced than for the longer set, with the former having a steeper gradient in Figure 2. The shorter set differs from the longer set mainly in its improved spatial coverage in the Pacific, which implies that the change in the NAO-temperature relationship is perhaps even more pronounced in the Pacific.

[18] We wish to examine how the correlation between the NAO and the local temperature changes with time, given the observed change in the NAO-NH20N relationship. Figure 3 shows maps of correlations between the 1870–2004 high-pass filtered DJFM NAO and HadCRUT2v gridded temperature data composited for the years when the NAO-NH20N correlation (Figure 2) is below its median value of 0.55 (Figure 3a) and above its median (Figure 3b). The difference between these two plots (Figure 3c) reveals that when the NAO-NH20N correlation is high, correlations are generally more positive over Eastern Europe, the central Atlantic and North America. Note that some of the regions with a positive change in correlation in Figure 3c are regions with a negative NAO-temperature correlation. This implies a weakening negative correlation in Figure 3b compared with Figure 3a, for example in the central North Atlantic. The hatching in Figure 3c indicates where the differences in the mean correlation of the two composites are significant using a t-test. Because of the high serial correlation in the running correlation time series, we assessed the significance of the difference in the composites by randomly resampling two equal blocks of correlations 1000 times and compared their difference to that obtained by compositing the years according to the time series in Figure 2. The shift in correlations between Figures 3a and 3b can be seen in the change in the probability density function (PDF) of correlations (not shown) across all grid points for the two composites. This shows that higher NAO-NH20N correlations are associated with a reduction in NAO-grid point temperature correlations in the range −0.5 to 0.2 and an increase in correlations above 0.2.

[19] Figures 3a and 3b indicate that there are many grid points with both positive and negative correlations. Therefore it is more prudent to look at NAO-temperature squared correlation (r^2) averaged across the hemisphere rather than correlations between NH average temperature and the NAO. This is so as not to cancel the effects of regions that are out-of-phase with regards variability associated with the NAO. Figure 4 illustrates the r^2 for running 31-year periods between the high-pass filtered NAO and HadCRUT2v calculated as a latitude-weighted average of all long-term grid points north of 20°N (Figure 1). This time series has high values in 1888, 1935 and 1983 and low values in 1921 and 1956. The general pattern is also very similar to that seen in Figure 2, with peaks in the early and later years and the lowest values in the early part of the 20th century, however in the 1940s, what is a trough in Figure 2 is the centre of broad peak in Figure 4 that extends from about 1920 to 1960. Also plotted in Figure 4 is the average NAO-temperature r^2 using the more spatially complete shorter data set. This shows generally lower values with a greater trough in 1956, implying that NAO-temperature correlations are generally lower in magnitude in the Pacific sector than in other longitudes around the hemisphere.

[20] There is a possibility that a few odd or erratic years are affecting the correlations because of the sensitivity of the Pearson correlation to extreme values. Therefore we recalculated the average NAO-temperature squared correlation but using the Spearman correlation, which is more resistant to outliers [*Press et al.*, 1986]. This series is also shown in Figure 4, and closely resembles the series calculated using the Pearson correlation. We also checked this by removing the years with the highest and lowest 5% of NAO and temperature values. A similar secular change in correlation was still evident. We thus conclude that the changing NAO-temperature correlation is not a product of several extreme years.

[21] We repeated this running correlation study using the HadISST data set [*Rayner et al.*, 2003] to confirm the above results with a quasi-independent data set, and to gain more detail over the oceans. HadISST is an update of the marine element of HadCRUT2v, and includes additional input observations and a different gridding scheme. The HadISST data set is a globally complete set that uses a two-stage reduced space optimal interpolation (RSOI) procedure, followed by superposition of high-quality gridded observations onto the reconstructions to restore local detail. Although data will naturally be less reliable over observation-sparse regions, by using the variability of large-scale empirical orthogonal functions (EOF), RSOI should give a best guess as to what the true state might have been.

[22] Figure 5 shows the 1870–2004 HadISST-NAO correlations as composites of years when the average NAO-temperature r^2 (Figure 4) is below its median (Figure 5a) and above its median (Figure 5b). Note that previously, with HadCRUT2v (Figure 3), we composited the years using the NAO-NH20N running correlation (Figure 2), whereas this time we use the NAO-temperature r^2 (Figure 4). The difference between these two composites (Figure 5c), shows that there are large areas where the correlations in Figure 5b are significantly more positive in the central North Pacific and North Atlantic and significantly more negative in the Eastern Pacific. Again, in some of the regions, a significant positive change in Figure 5c may correspond to a weaker negative correlation rather than a stronger positive correlation, for example the North Atlantic. The distribution of correlations for the two composites (not shown) shows that the change from Figure 5a to Figure 5b is a reduction of the number of points with low magnitude negative and positive correlations and a corresponding increase in moderate positive correlations. We can conclude that during periods when we see a higher squared NAO-temperature correlation, such as the late 19th century, 1930s and late 20th century, we see stronger positive correlations.

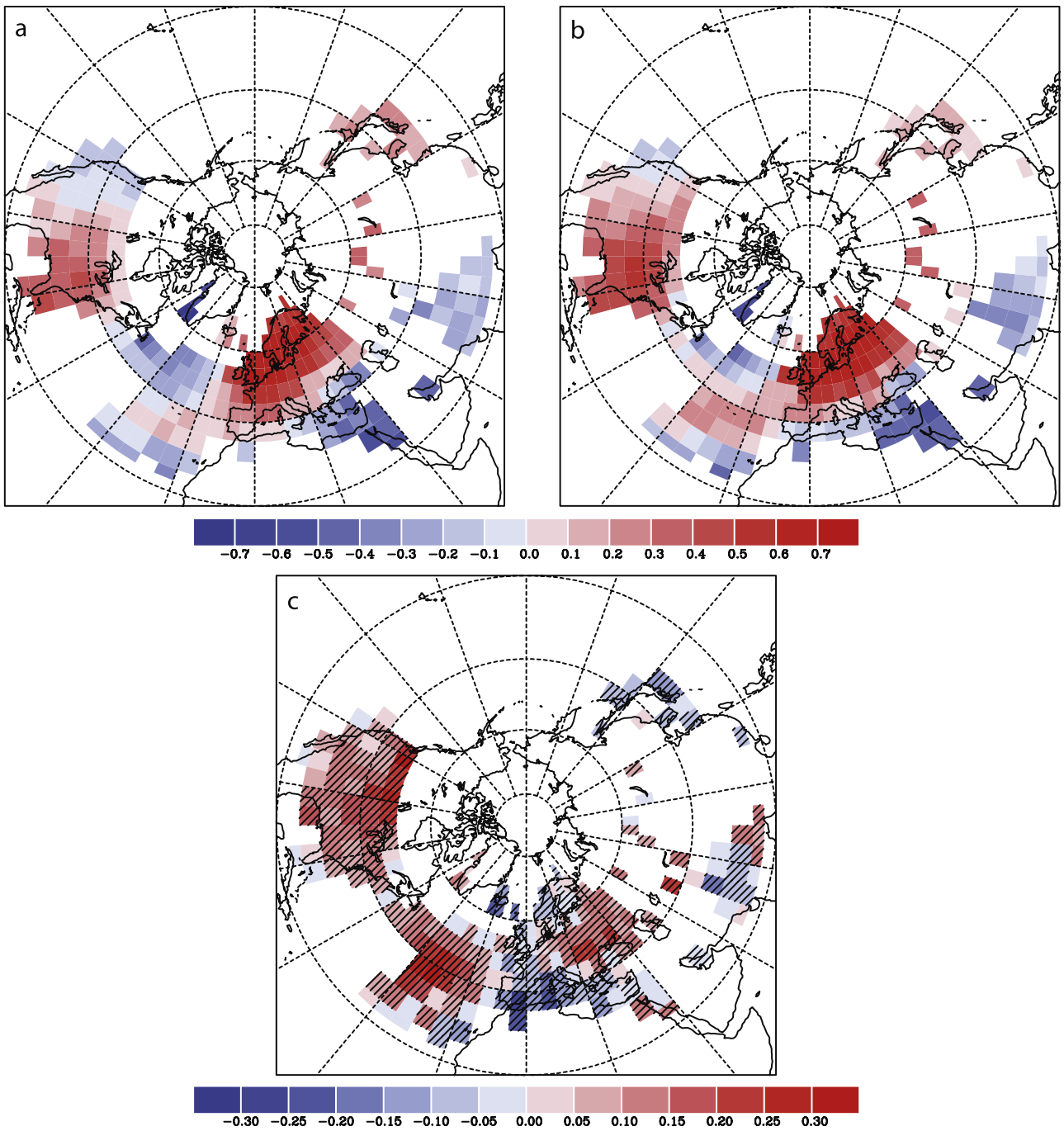

Figure 3. Composite of correlation between high-pass filtered DJFM NAO and HadCRUT2v gridded temperature for periods when correlation between the high-pass filtered NAO and NH average temperature (Figure 2) is (a) below its median and (b) above its median and (c) the difference of Figure 3b and Figure 3a. Hatching indicates regions where a grid point t-test is significant.

[23] Figure 6 shows the average NAO-HadISST r^2 calculated as a latitude-weighted average of Figure 5 for overlapping 31-year subperiods. Figure 6 reveals a significant trend ($p < 0.0001$) in the magnitude of correlations for Atlantic longitudes, and a strong "W" shaped pattern in correlation for the Pacific basin. The all-longitude average is similar to that seen in the HadCRUT2v data set (Figure 4) but with a more enhanced peak in the 1940s and troughs circa 1920 and 1960. Figure 6 shows that the low-frequency variability in the NH average NAO-temperature correlations is mainly due to changing correlations in the Pacific basin. This confirms the results of *Jones et al.* [2003], who found a multidecadal change in the correlations between the NAO and NH temperatures, but more constant NAO-European temperature correlations.

3. Changes in the Variance of Northern Hemisphere Sea Level Pressure

[24] *Raible et al.* [2001] and *Walter and Graf* [2002] concluded that during periods of enhanced decadal variability

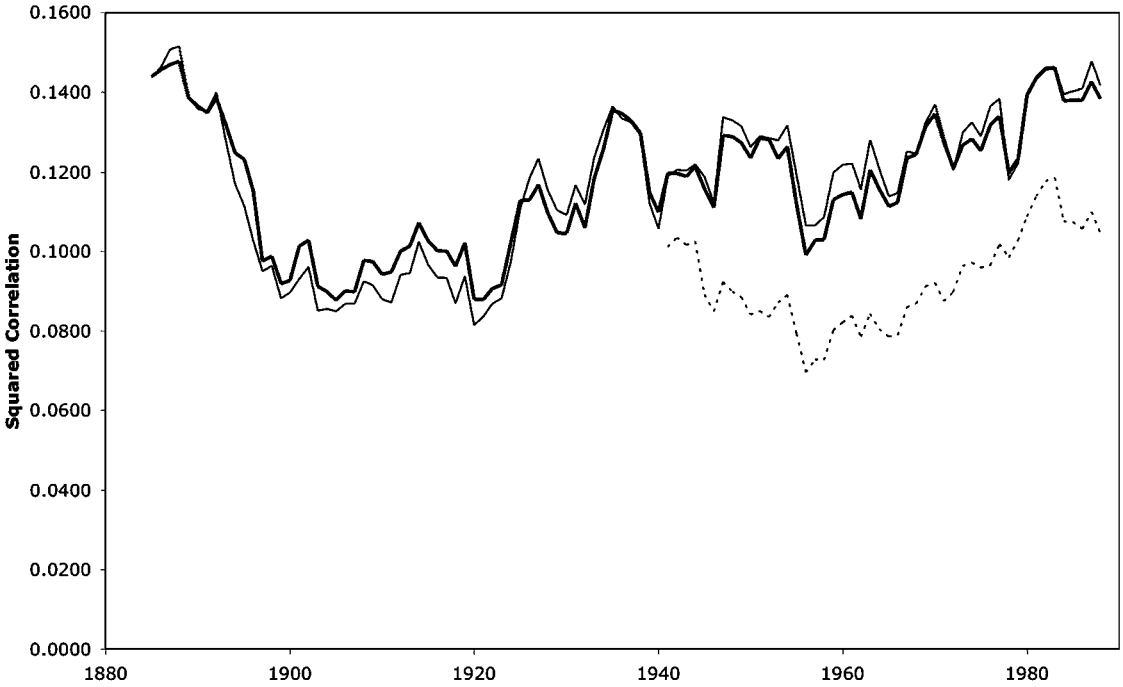

Figure 4. Latitude-weighted average r^2 for running 31-year periods between the high-pass filtered NAO and NH HadCRUT2v points (thick line) and using the square of the Spearman correlation (thin line). Also shown is the same analysis using the squared Pearson correlation for the shorter, more spatially complete data set (dashed line).

in the NAO, such as the later decades of the 20th century, the NAO had a stronger correlation with North Atlantic SSTs with a corresponding less active PNA pattern. Our own examination of the 31-year running variance of the DJFM NAO index (Figure 7, thick line) shows that it was about 50% higher in the late 19th and 20th centuries compared with the mid-20th century. This suggests that the reduced activity of the NAO in the mid-20th century might be a possible explanation as to why the NAO-NH20N correlation is weaker during this period (Figure 2). Also we found in section 2 that there was a strong W-shaped variation in NH average squared correlations of temperature and the NAO, mainly because of changes in the Pacific. One common index of the SLP in the North Pacific is the North Pacific Index (NPI) [*Trenberth and Hurrell*, 1994], which is the area-averaged pressure over the region 30–65°N and 160°E–140°W (see comparisons and extensions of the NPI and an Aleutian Low index from different sources (including HadSLP2) in the work by *Allan and Ansell* [2006]). An examination of the running variance of the NPI, also plotted in Figure 7 (thin line, calculated from HadSLP2 data) shows similarity with the W-shaped pattern in SLP-temperature average squared correlations (Figures 4 and 6). Therefore we wish to examine in more detail the changing NAO-temperature correlation in the context of the changing centre of SLP variance. Our justification for this approach, in addition to the above noted similarities, is based on the hypothesis that with less active SLP variability, one might expect a reduced influence on other climate parameters such as temperature.

3.1. Relationship Between Northern Hemisphere Temperature and Large-Scale Circulation Indices

[25] Before examining the changing SLP variability, we first examine the relationship between NH20N and other NH circulation indices as well as the SOI. We do this is in order to determine whether NH20N is responding to forcings other than the NAO as a possible explanation for the changing relationship with the NAO. Also we wish to see if the importance of the NPI suggested above can be determined objectively.

[26] *Hurrell* [1996] used multiple linear regression to model the 1935–1994 DJFM NH20N index as a function of the NAO, the Southern Oscillation Index (SOI) and the NPI. He showed that much of the warming in Europe and cooling in the northwest Atlantic could be explained by circulation changes, with the NAO accounting for 31% of the interannual variance of NH temperature. The SOI accounted for about 16%. The large correlation between the SOI and NPI (0.51) led to high standard errors in the estimated regression coefficients for the two indices.

[27] We repeated a multiple linear regression of the NH20N index using the NAO, SOI, NPI, Northern Annular Mode (NAM [*Thompson and Wallace*, 2000]) and Pacific Decadal Oscillation (PDO [*Mantua et al.*, 1997]). The availability of all the indices limited the analysis to the common period 1899–2002. Because of the high correlation of the predictors (Table 1), we used singular value decomposition to give a more robust solution to this numerically unstable least squares problem [*Press et al.*, 1986]. Since our prime aim was to model the high-frequency interannual variability of NH20N, we first high-

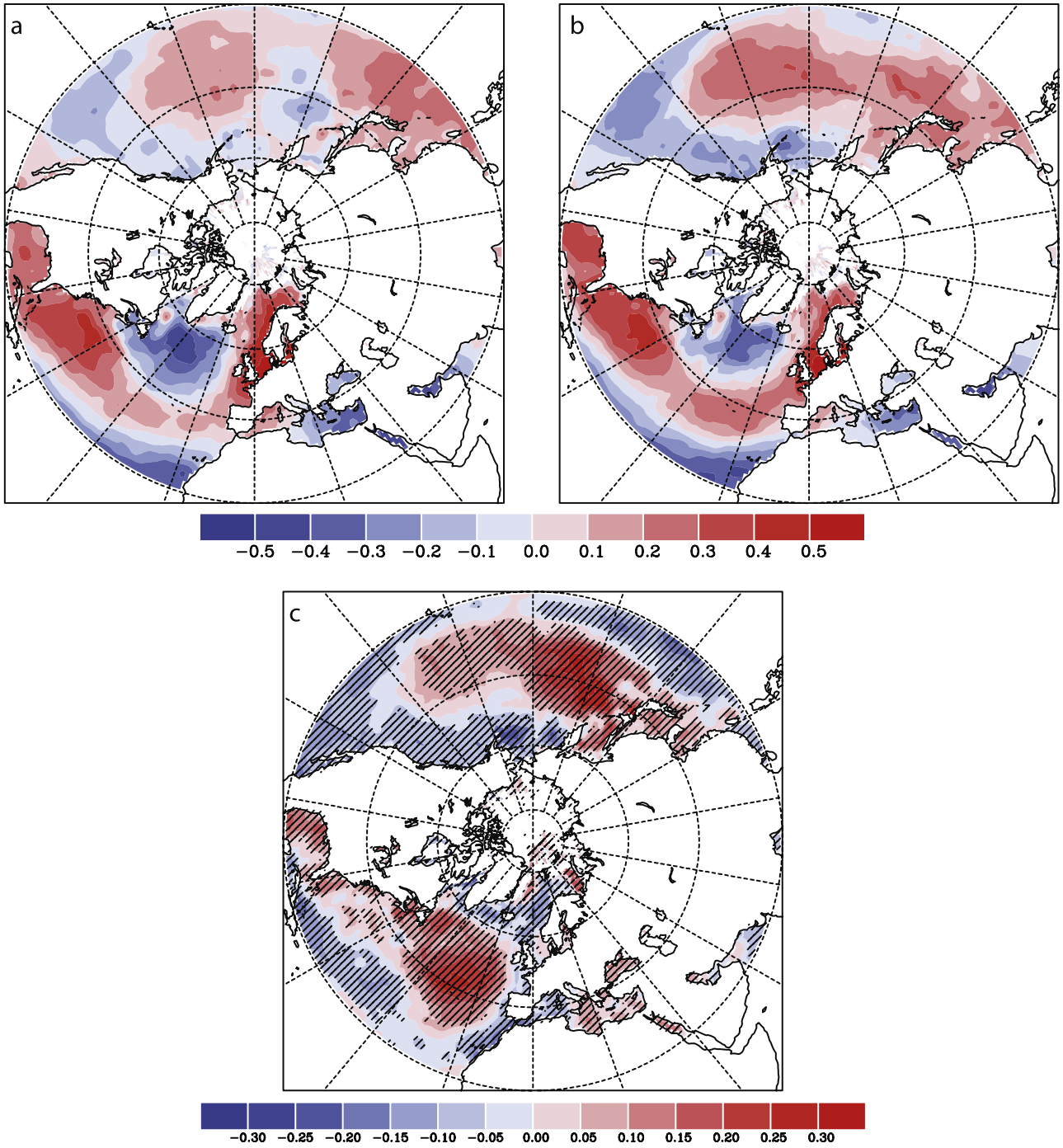

Figure 5. Composite of correlation between high-pass filtered DJFM NAO and HadISST gridded sea-surface temperature for periods when the average squared correlation between high-pass filtered NAO and HadCRUT2v temperature (Figure 4) is (a) below its median and (b) above its median and (c) the difference of Figure 5b and Figure 5a. Hatching indicates regions where a grid point t-test is significant.

pass filtered the DJFM averages of the predictor and predictands to remove frequencies with periods greater than 30 years. Fitting the NH20N index to all five predictors gave a correlation of 0.61 between the modeled and observed indices. However, this approach gives no indication of the best set of predictors and allows the possibility of overfitting the data by using too many predictors. We therefore selected the best predictor set by testing every combination of the five predictors ($2^5 - 1 = 31$ combinations) in a cross validation exercise to choose the best set. For each combination of predictors we selectively removed each year, fitted the model with the remaining years, then hindcasted the withheld year. By comparing the correlation between the hindcasted series and the observed we selected the best predictor set. This procedure selected the NAO and NPI as the best predic-

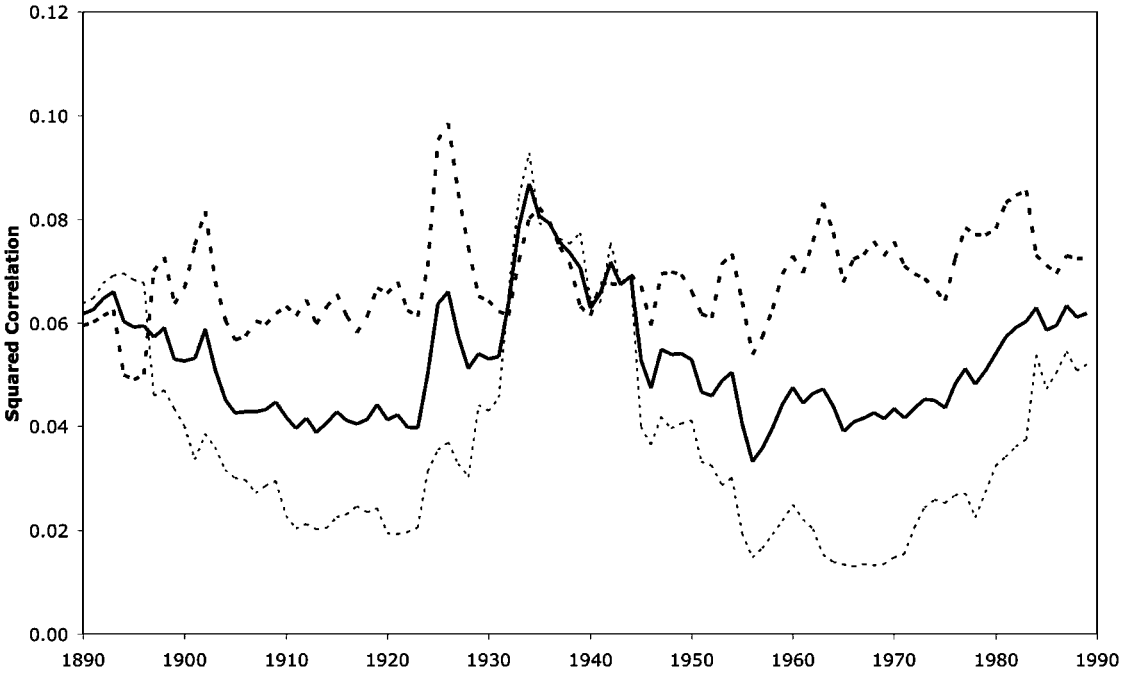

Figure 6. Latitude-weighted average r^2 for running 31-year periods between the high-pass filtered NAO and NH HadISST points for all longitudes (solid line), "Atlantic" longitudes 80°W to 0° (thick dashed line) and "Pacific" longitudes 120°E to 120°W (thin dashed line).

tors, resulting in a correlation of 0.58 between the hindcasted series and the observed. The partial correlations between NH20N and the NAO and NPI were 0.57 and −0.17 respectively.

[28] We can conclude from this regression analysis that the two most important SLP predictors for DJFM NH20N are the NAO and the NPI, indicative of SLP changes in the Atlantic and Pacific basins. The NAO is by far the

Figure 7. Running variance of the NAO and NPI indices.

Table 1. The 1899–2002 DJFM Correlation Between Five NH Climate Indices Used to Model NH20N

	NAO	SOI	PDO	NAM	NPI
NAO	1.00				
SOI	−0.02	1.00			
PDO	−0.17	−0.49	1.00		
NAM	0.73	0.10	−0.37	1.00	
NPI	0.16	0.47	−0.60	0.40	1.00

most important predictor with a much higher partial correlation than the NPI. The omission of the NAM indicates that there is no additional information available from this index, which has a high correlation with the NAO (0.73, Table 1.) and moderate correlations with the NPI (0.40). Likewise the SOI and PDO do not add additional skill as both are moderately correlated with the NPI (0.47 and −0.60). Note that our temperature coverage over the Pacific is relatively poor (Figure 1) which would lead to weaker relationships with the Pacific indices.

3.2. Relationship Between Northern Hemisphere Temperature and the Changing Spatiotemporal Pattern of Interannual Variance of Sea Level Pressure

[29] For this section, we use the recently compiled HadSLP2 data set (1850–2004) [*Allan and Ansell*, 2006]. This 5 × 5° gridded product is a compilation of land and ship observations, and includes superior spatial coverage to the previous version HadSLP1, which is an update to GMSLP2 [*Basnett and Parker*, 1997]. The globally complete HadSLP2 data set uses a similar RSOI gridding procedure to HadISST.

[30] Figure 8 shows the 1870–2004 31-year running variance of the high-pass filtered HadSLP2 data composited for periods when the 31-year running average NAO-HadCRUT2v r^2 (Figure 4) is below and above its median and the difference between the two composites (Figure 8c). Figure 8c shows that high NAO-HadCRUT2v r^2 is associated with enhanced SLP variance in the North Pacific and the region of northern Scandinavia and the Barents Sea, and reduced variance in the North Atlantic. This tendency is quantified in Figure 9, which shows the latitude-weighted average of the running variance for the HadSLP2 data for the entire NH north of 20°N as well as the "Atlantic" (80°W to 0°) and "Pacific" (120°E to 120°W) longitudes.

[31] Two features stand out in Figure 9: the tendency for higher variance through time (shown by the linear trend in the NH variance); and the large increase in variance in the Pacific from about 1920 to 1960. We suggest that the tendency to higher variance could be an artifact of data processing due to an increase through time in the quantity of observations in the gridded data, rather than a real feature. This would cause the gridded data to become less dependent on smooth RSOI gap filling through time thereby increasing their variance. On the other hand, an increase in the number of observations can have the opposite effect of smoothing out grid box averages as more observations are used in calculating the averages [*Jones et al.*, 2001], but this only applies to grid boxes that contain real observations and not those that are interpolated. We suspect that it is the former problem in this case. The trend is very significant ($p < 0.001$) for the whole NH north of 20°N. In addition, an even more significant trend exists in the NH average variance of the HadISST data (not shown), which is also compiled using RSOI. The HadCRUT2v data set, which does not use RSOI, does not contain a significant trend in variance. To examine this further we have looked at the running variance of three stations in the Atlantic that are commonly used to create NAO indices: Gibraltar, Ponta Delgada and Reykjavik (not shown). Only Gibraltar has an increasing trend in variance, which is not significant. The large jump in variance from 1920 to 1960 in the Pacific, however, cannot be explained by changes in the observation network. The fact that it matches the period when there is a jump in the NAO-HadCRUT2v r^2 (Figure 4) suggests that this is a real feature.

[32] The jump in SLP variance in the Pacific in 1920–1960 is particularly interesting as during this period the variance in the Atlantic remains constant and even reduces slightly up until 1940. Variances in the Atlantic and Pacific sectors run in parallel up until 1900, where they diverge and remain out-of-phase for the rest of the record. The correlation for the two sectors is −0.391 ($p < 0.07$). Because of the high serial correlation in both series, which are calculated from overlapping 31-year periods, we calculated the significance of this correlation using the "random phase" method of *Ebisuzaki* [1997]. Although not quite significant at the 95% level, Figure 9 illustrates the low-frequency out-of-phase behavior in the two domains; when variance increases in the Pacific it decreases in the Atlantic.

[33] To confirm the observed reduction in SLP variance in the Atlantic we examined the running variance of the NAO index. Figure 7 reveals that this does indeed show a decline in the middle part of the record similar to the Atlantic-wide decline (Figure 9). This was also examined by *Walter and Graf* [2002] who, through wavelet analysis, concluded that reduced decadal variability was the cause of the reduced variance. However, a high-pass-filtered version of the NAO index also shows a similar decline in variance. Figure 7 also shows the running variance for the NPI index, which is very similar to the Pacific sector running variance of Figure 9.

[34] Also notable in Figure 9, is the similarity between the W-shaped changes in SLP variance and the average NAO-temperature r^2 from Figure 4. The correlation between the average variance across the entire NH and the average NAO-temperature r^2 is 0.67 ($p < 0.002$, taking into account autocorrelation in the series). Therefore about 40% of the changes in the NH NAO-HadCRUT2v r^2 can be explained by changes in the total NH SLP variance.

[35] Our division of the NH into the Atlantic and Pacific basins was based purely on a cursory examination of Figure 8. We have quantified the changing variance of NH SLP by performing a Principal Component Analysis (PCA) on the linear-detrended and latitude-weighted running variance of DJFM averaged SLP based on the covariance matrix. PCA has been used many times on boreal winter SLP data to reveal the NAO (in the Atlantic sector) or the annular Northern Annular Mode/Arctic Oscillation (NAM; using the entire hemisphere) as the first PC [*Trenberth and Paolino*, 1981], which reflects interannual movements of mass from the high to midlat-

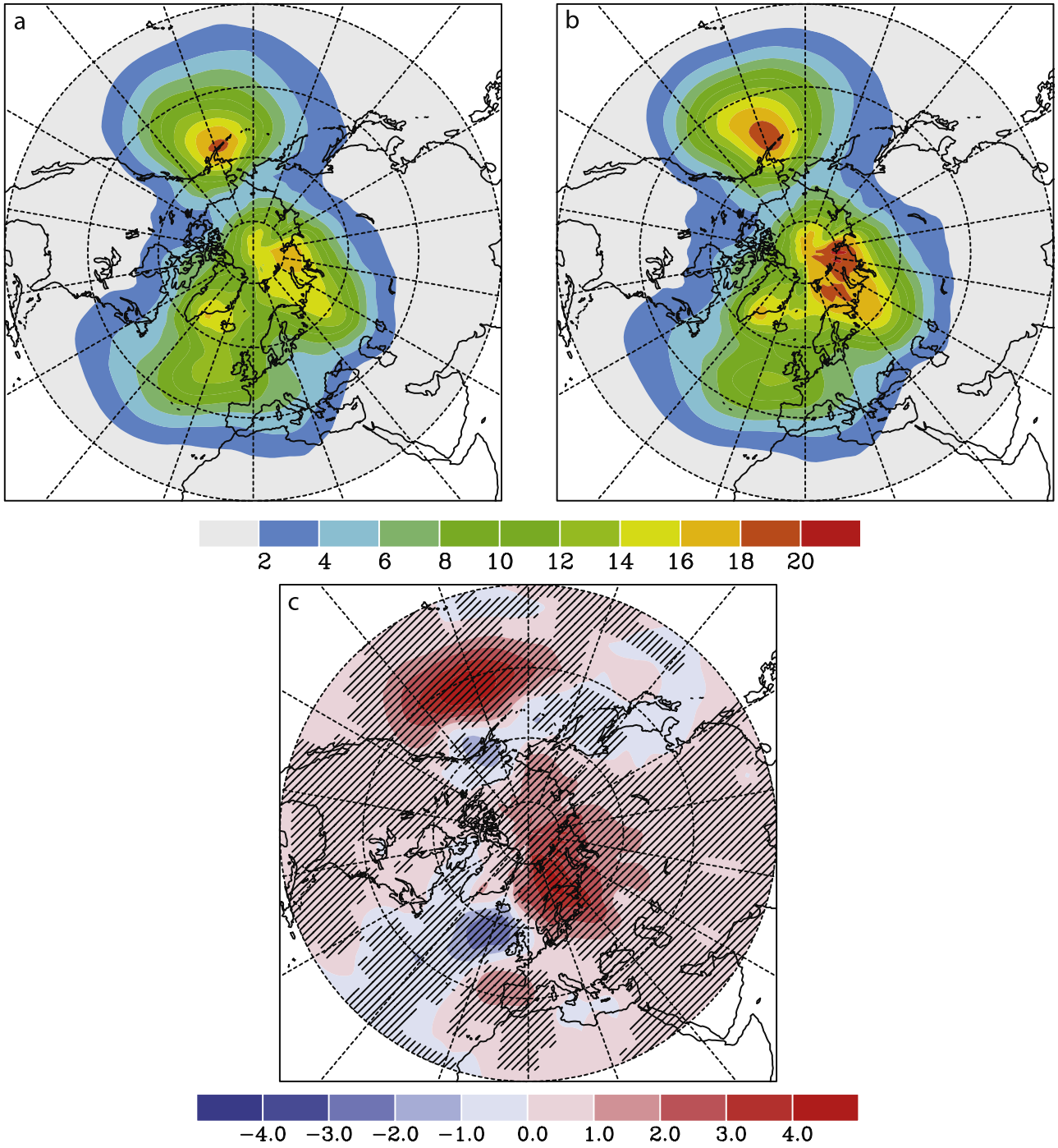

Figure 8. Composite of HadSLP2 variance for periods when average squared correlation between high-pass filtered NAO and HadCRUT2v temperature (Figure 4) is (a) below its median and (b) above its median and (c) the difference of Figure 8b and Figure 8a. Hatching indicates regions where a grid point t-test is significant.

itudes. However, our aim is to determine the changing spatiotemporal pattern of interannual variance. In other words, the aim of the PCA here is to isolate regions that have seen large coherent changes in the variance of winter SLP through time. The PCA was carried out by performing a singular value decomposition of the matrix of anomalies of variance, after the variance at each grid point was first divided by the cosine of the latitude. All PCs presented are unrotated as we are primarily interested in finding the component that maximizes the variance (of changing SLP variability) across the entire region, rather than finding localized modes that are derived from common rotations.

[36] Figure 10 shows the second principal component (PC) of NH SLP running variance together with the average NAO-HadCRUT2v r^2 (from Figure 4). The correlation between the two series is 0.70 ($p < 0.001$). We have also

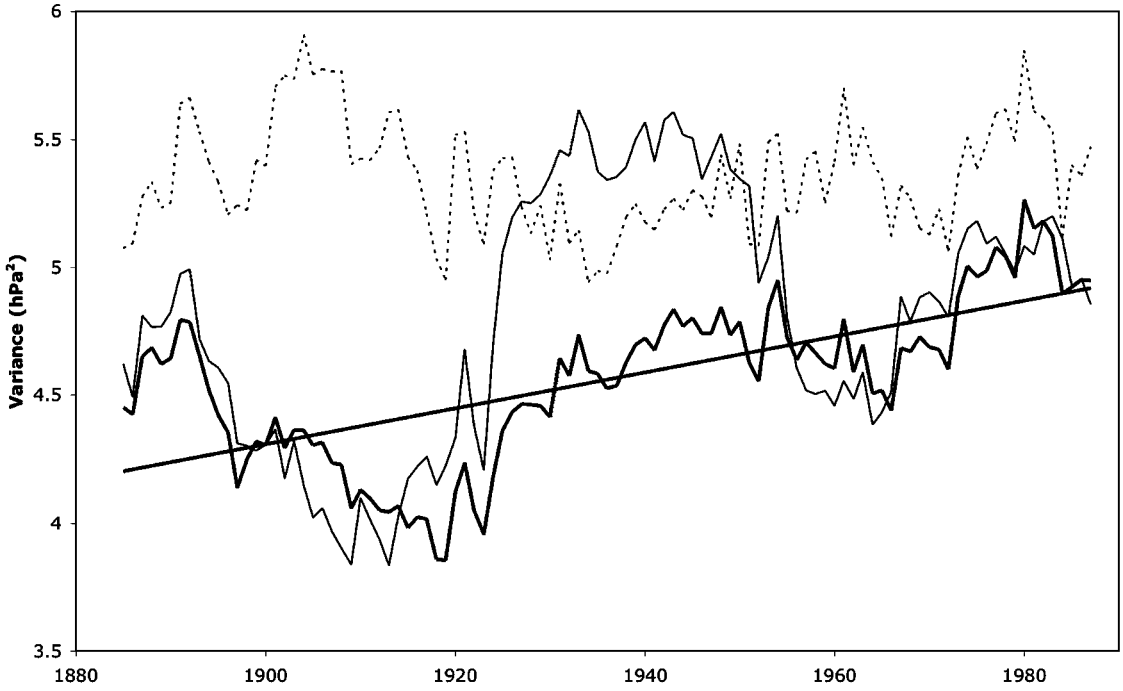

Figure 9. Latitude-weighted average of the variance of high-pass filtered SLP north of 20°N for a running 31-year window for the entire NH (thick solid line), the Atlantic sector (thin dashed line) and the Pacific sector (thin solid line). The linear trend of NH variance is shown as a thick solid line.

Figure 10. Second principal component of running 31-year DJFM SLP variance (thick solid line, RHS axis). Also shown is the latitude-weighted average r^2 for running 31-year correlations between the NAO and NH HadCRUT2v points (thin solid line, same as Figure 4, RHS axis) and the same but using the AO instead of NAO (thin dashed line, RHS axis).

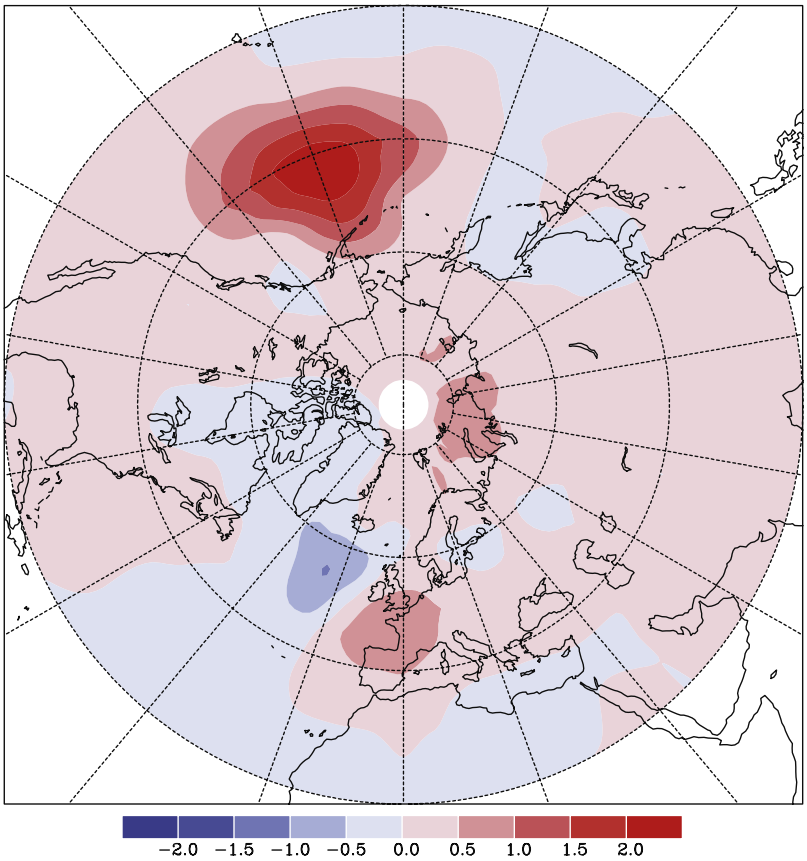

Figure 11. Factor loadings for the second PC of running variance of HadSLP2.

included the latitude-weighted average NAM-HadCRUT2v r^2, where NAM is defined as the first PC of NH DJFM-average MSLP. This has an even higher correlation with our second PC of NH SLP variance (0.81, $p < 0.001$). We would expect the NAM- HadCRUT2v r^2 to have a higher correlation with our PC than when using the NAO as the NAM is indicative of SLP variance changes across the entire hemisphere rather than just the Atlantic. The map of factor loadings for the second PC of HadSLP2 variance is shown in Figure 11, which is remarkably similar to the composites of HadSLP2 variance depending on the average NAO-HadCRUT2v r^2 (Figure 8). The pattern correlation between the two figures is 0.70 ($p < 0.01$, allowing for autocorrelation in the spatial patterns). Large positive loadings over the Pacific coincide with smaller negative loadings over the Atlantic, highlighting the previously mentioned out-of-phase change in variance across the two basins. PC2 explains 24.8 percent of the total variance of running variance of NH SLP. The fact that correlations between the NAO and NH temperature are higher when SLP variance in the Pacific is higher implies that SLP variability in the Pacific during this time is correlated with the NAO. If this were not the case we would expect the NAO-HadCRUT2v correlations to be reduced when the SLP variance in the Pacific is greater.

[37] The first PC of running variance is shown in Figure 12 with its loadings in Figure 13. This PC explains 43.4 percent of the total variance of running variance of NH SLP. The PC changes from positive values at the start of the period to negative values in the 1920s to 1950s then reverses sign again. This corresponds to a reduction of variance in the 1920s to 1950s for those regions with positive loadings in Figure 13 and an increase for those regions with negative loadings. The strong centre of negative loadings over the UK suggests that this region saw a strong increase in the variance of boreal winter SLP in the early to mid-20th century. This corresponds with reduced variance during the same period over the high latitudes of the North Atlantic that have large positive loadings. The two positive centers in the midlatitudes and high latitudes of the North Atlantic occur near the Iceland low and the Azores High, the poles of the NAO. Therefore one would expect similarity in the corresponding PC and the running variance of the NAO (Figures 12 and 7, respectively). Accordingly this PC also helps us explain the changing NAO-NH20N correlations as it highlights the greatly reduced variance of the NAO during the early mid-20th century. Moderate negative loadings over the Pacific also indicate an increase in the variance of SLP in this region during those years. We note that the center of negative loadings in the Pacific in PC1 (Figure 13) is further northeast and weaker compared with the center in PC2 (Figure 11).

[38] We repeated the PCA of SLP variance for the entire globe. The loadings of the first PC are given in Figure 14 and are very similar to Figure 11, with an NH pattern correlation between the two of 0.67 ($p < 0.01$, allowing for autocorrelation). The corresponding PC score series (not shown) is very similar to Figure 12, with a correlation

Figure 12. First principal component of running 31-year DJFM SLP variance.

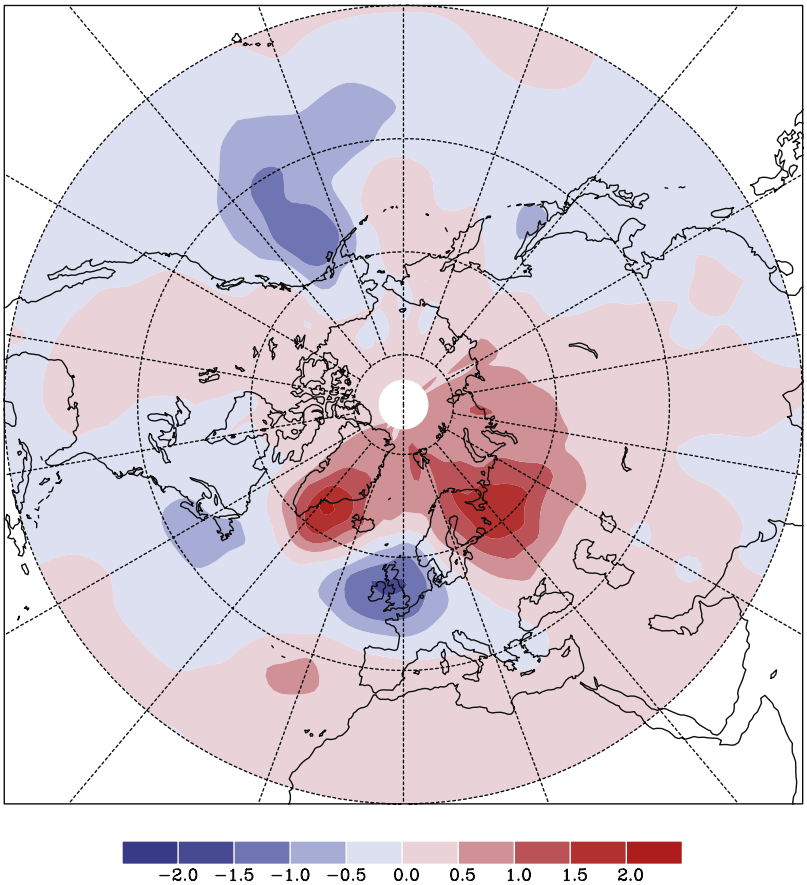

Figure 13. Factor loadings for the first PC of running variance of HadSLP2.

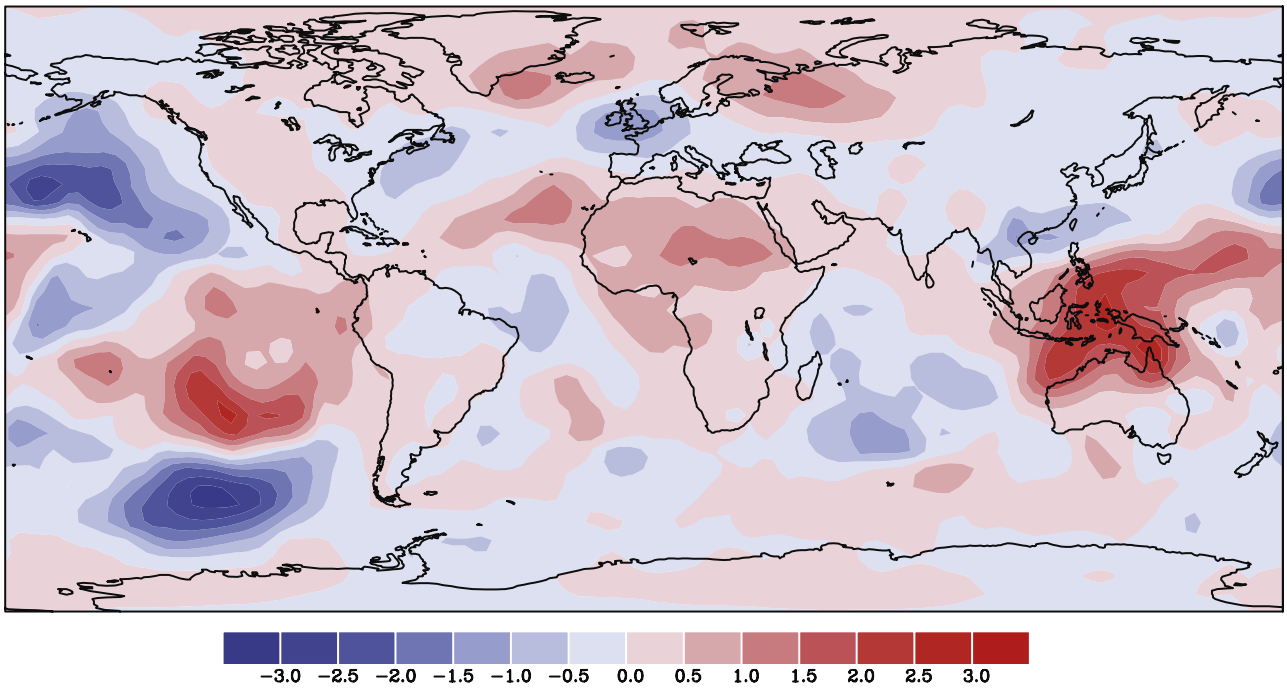

Figure 14. As for Figure 13 but for global data.

between the two of 0.70 ($p < 0.01$). Three important features are evident in Figure 14. First, the high positive loadings centered over the Eastern Tropical Pacific and the Maritime Continent indicate that this PC largely reflects changes in the variance of the atmospheric component of tropical Pacific oscillations such as the El Niño–Southern Oscillation (ENSO). We confirmed this by comparing the PC score series with the 31-year running variance of the DJFM SOI; the two are correlated at 0.86 ($p < 0.01$). Correlations with the running variance of the DJFM Pacific Decadal Oscillation (PDO [*Mantua et al.*, 1997]) are much lower (0.07). The PDO is the leading PC of monthly SSTs in the North Pacific. Although it contains some correlation with the tropical Pacific, it is more indicative of high-latitude variability of SST. The PDO contains a strong decadal signal that is highly correlated with the Interdecadal Pacific Oscillation (IPO [*Folland et al.*, 1999, 2002; *Power et al.*, 2006]), calculated as the leading PC of low-pass-filtered global SST. The sign of the loadings of our leading PC of SLP variance, combined with the PC scores, implies that SLP variance of the tropical Pacific was much lower in the middle of the 20th century compared with the late 19th to early 20th century and late 20th century, confirming work of many previous studies [*Allan et al.*, 1996; *Newman et al.*, 2003; *Torrence and Compo*, 1998]. Note that in Figure 14 the loadings in the eastern and western Pacific are the same sign, unlike the well-known out-of-phase movement of mass in the Pacific related to ENSO. This is because our PCA analyzed changing variance of SLP and not the changing SLP itself. Therefore changes in ENSO variance were due to changes in both poles of the Southern Oscillation.

[39] Second, the high negative loadings in the North and South Pacific indicate that increasing variance in the higher latitudes of the ocean basin in the mid-20th century was out-of-phase with the reduction in the tropics. Observations were very sparse in the far South Pacific for much of the record, so the high negative loadings in this region are probably dubious (see discussion by *Allan and Ansell* [2006]). However, the NH has better coverage. This out-of-phase behavior implies that, with largely reduced Eastern Pacific tropical SST variability in the mid-20th century, the high latitudes were free to respond to other forcings or their own natural atmospheric modes. A similar PCA of SST variance (not shown) shows high loadings only in the eastern Pacific, indicating that high-latitude SST forcing was not responsible for changes in the high-latitude SLP variance.

[40] Third, as previously noted in our earlier NH PCA of variance, the first PC was indicative of reduced variance of the NAO during the mid-20th century. The global analysis suggests that this corresponded to a similar change in the variance of ENSO. The loading pattern (Figure 14) of the first PC shows continuous loadings of the same sign stretching from the eastern Pacific northeastward into the subtropical North Atlantic. We suggest, therefore, that the changes in NAO variance might be the result of the changing ENSO variance. We plan to investigate this link more fully in future work.

3.3. Changing NAO-Temperature Correlation in Relation to the Sectoral Symmetry of Sea Level Pressure Variability

[41] The results of our analyses have implications for the debate on whether high-latitude meridional wintertime SLP variability in the NH is best expressed by the annular NAM or the Atlantic-only NAO. This discussion has been most prominent in the literature in recent years, with strong arguments from both sides supporting the hemispheric [*Wallace*, 2000; *Wallace and Thompson*, 2002] and sectoral viewpoints [*Ambaum et al.*, 2001; *Deser*, 2000; *Dommenget*

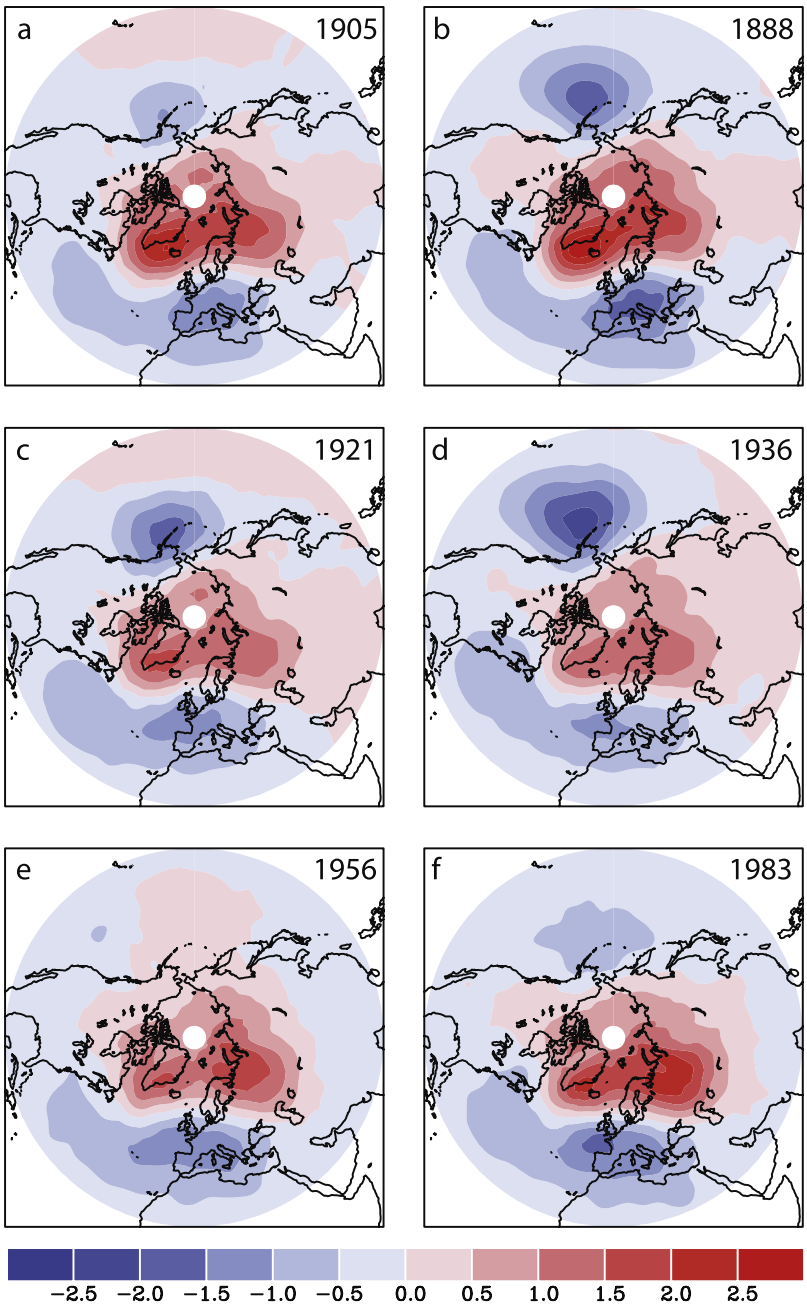

Figure 15. Pattern of loadings for 1st PC of DJFM mean SLP for selected 31-year periods.

and Latif, 2002]. The annular mode paradigm derives from the fact that the first unrotated PC of NH SLP is annular in structure, with dominant centers over the Atlantic and Pacific domains. The contrary NAO theory points out the problems in interpreting EOFs as real climate modes, as well as the lack of correlation between the Pacific and Atlantic centers. The NAO adherents argue that the two basins appear in the first PC only because they both share an out-of-phase component with the Arctic.

[42] Our contribution to this debate derives from the analysis of the changing pattern of SLP variability over time. We showed that, while the NAO has undergone a change in interannual variance during the 20th century, it is very different to the changing variance in the Pacific (Figure 9). The second PC of our PCA of variance revealed the main centre of action to be a monopole centered over the North Pacific, with little high-latitude loading (Figure 11). This result points toward a Pacific centre that behaves independently of the Atlantic. However, there is one key issue that clouds the argument: we showed that it was during periods when variance was high in the Pacific that the relationship between the NAO and NH temperature was strongest, in particular the middle of the 20th century. This implies that when variance was high in the Pacific, the variability was in-phase with the Atlantic. The answer to this quandary probably lies in the complex and chaotic nature of atmospheric dynamics, showing very different behavior at different times. We have quantified this by

performing a covariance matrix PCA of DJFM mean SLP for running 31-year periods. We chose not to rotate the PCs so as to retain the maximum variance in the first PC. The pattern of loadings for the dominant first PC changes largely through time, but in all cases is a reflection of the NAM/NAO movement of mass between the Arctic and lower latitudes. The pattern of loadings for the first PC varies largely through time in the degree to which the Pacific is in phase with the Atlantic. Figure 15 shows the pattern of loadings for 6 selected 31-year periods. The periods were chosen by an examination of the strength of the NAO-HadCRUT2v relationship (Figure 4). Three of the periods are indicative of when the NAO-HadCRUT2v relationship is weak (Figures 15a, 15c, and 15e) and three periods indicate when it is strong (Figures 15b, 15d, and 15f). A strong NAO-HadCRUT2v relationship corresponds to periods when the Pacific centre is in-phase with the Atlantic or the pattern is more annular. During the periods with a weaker NAO-HadCRUT2v relationship there are loadings in the Pacific of mixed sign. Thus our study suggests that at times NH winter SLP variability behaves as both a sectoral and an annular mode.

4. Discussion and Conclusion

[43] Several conclusions derive from the analysis in sections 2 and 3. We examined the changing correlation between the NAO and NH temperature north of 20° (NH20N). We confirmed that there has been a change in the midfrequency and high-frequency (periods less than 30 years) NAO-NH20N correlations which is not caused by a change in the station network or several outlying years, supporting the work of *Jones et al.* [2003]. When the NAO-NH20N correlation is higher, there is an increase in the area where the local temperature has correlations with the NAO of between 0.2 to 0.6, and a decrease in the area with correlations −0.4 to 0.2. This is manifest as a positive shift in the distribution of correlations, although the proportion of grid points with the highest and lowest correlations (the upper and lower tails of the distribution of correlations) stays the same. The mix of positive and negative correlations between the NAO and local temperature meant that it was more prudent to look at average squared correlations (r^2) to examine the changing strength of the NAO-temperature relationship. Simply averaging the temperature across all grid points and correlating this with the NAO would reduce the NAO temperature signal because of the competing positive and negative correlations. By examining the change in the NAO-temperature r^2, we showed there has been a strong decadal "W"-shaped pattern in the Pacific but a more constant relationship in the Atlantic. This supported earlier work [*Jones et al.*, 2003] showing that the correlation between European winter temperatures and the NAO have remained fairly constant, while the correlations with the hemispheric average temperature have shown marked decadal change.

[44] In seeking causes for the observed change in NAO teleconnections, we first modeled NH average temperature as a linear function of several NH climate indices and the SOI. This led to the conclusion that NH temperature is mainly dependent on the NAO and the North Pacific Index (NPI) to a lesser degree. We therefore sought to explain the changing teleconnections by examining the changing variance of NH SLP. Our examination of the link between changing correlations and changing SLP variance was based on the simple premise that, with less active SLP variability, one might expect less active teleconnections. We showed that SLP variance had indeed changed markedly through time, especially in the North Pacific. The variance in the Atlantic showed less change, but interestingly was slightly negatively correlated with the Pacific. This implies a movement of the centers-of-action between the Atlantic and Pacific basins. Importantly, in support of our variance-teleconnection hypothesis, the changes of NH total SLP variance accounted for about 40% of the changing NAO-temperature relationship.

[45] To gain a more precise definition of the spatiotemporal structure of SLP variance, we performed a PCA of the running variance at each grid point. This is the first application of PCA to running variance in climate studies that the authors are aware of. Perhaps this approach is stretching the limits of s-mode PCA in its use of strongly autocorrelated data derived from running 31-year periods with few degrees of freedom and many grid points. However, PCA has been used in the past with autocorrelated data such as 13-year low-pass-filtered SST data to reveal the IPO [*Folland et al.*, 1999, 2002; *Power et al.*, 2006]. Additionally, we were careful that all our calculations of statistical significance took into account the high autocorrelation. The resulting PCs in our analysis agree strongly with our earlier findings concerning the spatiotemporal nature of variance. Also, the global PCA revealed a tropical Pacific-dominated first component with a score series highly correlated with the running variance of the SOI. The second PC explained 49% of the changing NH NAO-temperature relationship due to its corresponding loadings being dominated by the Pacific where the largest changes in SLP variance have occurred. The first PC (explaining 24.8% variance) was indicative of the changing variance of the low and high latitudes of the North Atlantic (close to the two poles of the NAO) and their out-of-phase changes with respect to the midlatitudes. While this change in the variance of the NAO poles has probably had an impact on the NAO teleconnections (compare Figures 2 and 12), it is independent of the large changes in the Pacific.

[46] The role of ENSO and the PDO/IPO in the changing SLP variability picture was revealed by the first PC of running variance being indicative of the changing strength of variability over the tropical Pacific. We therefore suggested that it might be changes in the variability of ENSO that have caused concurrent changes in the variance of the NAO. We plan to address this in more detail in a future study. Our PCA analysis indicated that variability of the Aleutian Low was strongest when ENSO was weakest. Perhaps it is only coincidence that leads to the fact that when the variance of the tropical Pacific is at it lowest during 1920–1950 (Figure 12), the variance of the North Pacific increases and becomes correlated with the NAO. Recent work by *Bronnimann et al.* [2007], examining ENSO influence across the European domain over the last 500 years in instrumental and reconstructed data, indicates that ENSO influence on Europe is strongest and most coherent when the PDO (reflecting mainly North Pacific conditions) is in-phase with boreal winter ENSO events in the following year. However, our two PCs of SLP variance

(Figures 10 and 12) are orthogonal, and so there is no relationship between the two. On the other hand, past studies linking the equatorial region and North Pacific give strength to the hypothesis. The relationship between atmospheric behavior over the equatorial and North Pacific regions has received much attention since *Bjerknes* [1969] reported that during El Niño events the Aleutian Low tends to become stronger and move southeastward of its normal position. The intensity of the Aleutian Low is measured by the North Pacific Index (NPI) [*Trenberth and Hurrell*, 1994]. Calculating the 31-year running variance for the NPI, based on the HadSLP2 data, gives rise to an index that is highly correlated ($r = 0.86$, $p < 0.02$) with our second PC of running variance. This is to be expected, since the loadings for our PC are dominated by the North Pacific. Therefore studies that have linked variability in the equatorial Pacific to the strength of the Aleutian Low imply that during times of reduced variability in the tropics, one would expect less influence on the North Pacific.

[47] Finally, our study has important implications for studies relying on stable teleconnections, including statistical downscaling and seasonal forecasting. Our results suggest that seasonal predictions of atmospheric circulation from SST patterns may be subject to interdecadal variations of skill. Predictions are likely to need to take account of tropical phenomena, such as ENSO/PDO/IPO, as well as extratropical SST features.

[48] **Acknowledgments.** This study was made with financial support by the Office of Science, U.S. Department of Energy, under grant DE-FG02-98ER62601. Rob Allan and Tara Ansell were supported by the U.K. Government Meteorological Research (GMR) programme, and this paper is U.K. Crown Copyright.

References

Allan, R. J., and T. J. Ansell (2006), A new globally complete monthly historical gridded mean sea level pressure data set (HadSLP2): 1850–2004, *J. Clim.*, *19*, 5816–5842.

Allan, R. J., J. A. Lindesay, and D. E. Parker (1996), *El Nino Southern Oscillation and Climatic Variability*, 405 pp., CSIRO Publ., Melbourne, Vic., Australia.

Ambaum, M. H. P., B. J. Hoskins, and D. B. Stephenson (2001), Arctic Oscillation or North Atlantic Oscillation?, *J. Clim.*, *14*, 3495–3507.

Basnett, T., and D. E. Parker (1997), Development of the Global Mean Sea Level Pressure Data Set GMSLP2, *Clim. Res. Tech. Note 79*, 16 pp., Hadley Cent., Met Off., Bracknell, U. K.

Bjerknes, J. (1969), Atmospheric teleconnections from the equatorial Pacific, *Mon Weather Rev.*, *97*, 163–172.

Bronnimann, S., E. Xoplaki, C. Casty, A. Pauling, and J. Luterbacher (2007), ENSO influence on Europe during the last centuries, *Clim. Dyn.*, *28*, 181–197, doi:10.1007/s00382-006-0175-z.

Cook, E. R. (2003), Multi-proxy reconstructions of the North Atlantic Oscillation (NAO) Index: A critical review and a new well-verified winter NAO index reconstruction back to AD 1400, in *The North Atlantic Oscillation: Climatic Significance and Environmental Impact*, *Geophys. Monogr. Ser.*, vol. 134, edited by J. W. Hurrell et al., pp. 63–79, AGU, Washington, D. C.

Cullen, H. M., A. Kaplan, P. A. Arkin, and P. B. Demenocal (2002), Impact of the North Atlantic Oscillation on Middle Eastern climate and streamflow, *Clim. Change*, *55*, 315–338.

Deser, C. (2000), On the teleconnectivity of the "Arctic Oscillation," *Geophys. Res. Lett.*, *27*, 779–782.

Dommenget, D., and M. Latif (2002), A cautionary note on the interpretation of EOFs, *J. Clim.*, *15*, 216–225.

Ebisuzaki, W. (1997), A method to estimate the statistical significance of a correlation when the data are serially correlated, *J. Clim.*, *10*, 2147–2153.

Feldstein, S. B. (2002), The recent trend and variance increase of the annular mode, *J. Clim.*, *15*, 88–94.

Folland, C. K., D. E. Parker, A. Colman, and R. Washington (1999), Large scale modes of ocean surface temperature since the late nineteenth century, in *Beyond El Nino: Decadal and Interdecadal Climate Variability*, edited by A. Navarra, pp. 73–102, Springer, New York.

Folland, C. K., et al. (2001), Observed climate variability and change, in *Climate Change 2001: The Scientific Basis—Contribution of Working Group I to the Third Assessment Report of the Intergovernmental Panel on Climate Change*, edited by J. T. Houghton et al., pp. 99–181, Cambridge Univ. Press, New York.

Folland, C. K., J. A. Renwick, M. J. Salinger, and A. B. Mullan (2002), Relative influences of the Interdecadal Pacific Oscillation and ENSO on the South Pacific Convergence Zone, *Geophys. Res. Lett.*, *29*(13), 1643, doi:10.1029/2001GL014201.

George, D. G., S. C. Maberly, and D. P. Hewitt (2004), The influence of the North Atlantic Oscillation on the physical, chemical and biological characteristics of four lakes in the English Lake District, *Freshwater Biol.*, *49*, 760–774.

Haylock, M. R., and C. M. Goodess (2004), Interannual variability of European extreme winter rainfall and links with mean large-scale circulation, *Int. J. Climatol.*, *24*, 759–776.

Hurrell, J. W. (1996), Influence of variations in extratropical wintertime teleconnections on Northern Hemisphere temperature, *Geophys. Res. Lett.*, *23*, 665–668.

Hurrell, J. W., Y. Kushnir, G. Ottersen, and M. Visbeck (2003), An overview of the North Atlantic Oscillation, in *The North Atlantic Oscillation: Climatic Significance and environmental impact*, edited by J. W. Hurrell et al., pp. 1–36, AGU, Washington, D. C.

Jevrejeva, S., J. C. Moore, and A. Grinsted (2003), Influence of the Arctic Oscillation and El Niño-Southern Oscillation (ENSO) on ice conditions in the Baltic Sea: The wavelet approach, *J. Geophys. Res.*, *108*(D21), 4677, doi:10.1029/2003JD003417.

Jones, P. D., and A. Moberg (2003), Hemispheric and large-scale surface air temperature variations: An extensive revision and an update to 2001, *J. Clim.*, *16*, 206–223.

Jones, P. D., T. Jonsson, and D. Wheeler (1997), Extension to the North Atlantic Oscillation using early instrumental pressure observations from Gibraltar and south-west Iceland, *Int. J. Climatol.*, *17*, 1433–1450.

Jones, P. D., M. New, D. E. Parker, S. Martin, and I. G. Rigor (1999), Surface air temperature and its changes over the past 150 years, *Rev. Geophys.*, *37*, 173–199.

Jones, P. D., T. J. Osborn, K. R. Briffa, C. K. Folland, E. B. Horton, L. V. Alexander, D. E. Parker, and N. A. Rayner (2001), Adjusting for sampling density in grid box land and ocean surface temperature time series, *J. Geophys. Res.*, *106*, 3371–3380.

Jones, P. D., T. J. Osborn, and K. R. Briffa (2003), Pressure-based measures of the North Atlantic Oscillation (NAO): A comparison and an assessment of changes in the strength of the NAO and its influence on surface climate parameters, in *The North Atlantic Oscillation: Climatic Significance and Environmental Impact*, edited by J. W. Hurrell et al., pp. 51–62, AGU, Washington, D. C.

Mantua, N. J., S. R. Hare, Y. Zhang, J. M. Wallace, and R. C. Francis (1997), A Pacific interdecadal climate oscillation with impacts on salmon production, *Bull. Am. Meteorol. Soc.*, *78*, 1069–1079.

Newman, M., G. P. Compo, and M. A. Alexander (2003), ENSO-forced variability of the Pacific decadal oscillation, *J. Clim.*, *16*, 3853–3857.

Osborn, T. J., K. R. Briffa, S. F. B. Tett, P. D. Jones, and R. M. Trigo (1999), Evaluation of the North Atlantic Oscillation as simulated by a coupled climate model, *Clim. Dyn.*, *15*, 685–702.

Power, S., M. Haylock, R. Colman, and X. Wang (2006), Asymmetry in the Australian response to ENSO and the predictability of inter-decadal changes in ENSO teleconnections, *J. Clim.*, *19*, 4755–4771.

Press, W. H., B. P. Flannery, S. A. Teukolsky, and W. T. Vetterling (1986), *Numerical Recipes: The Art of Scientific Computing*, 818 pp., Cambridge Univ. Press, New York.

Raible, C. C., U. Luksch, K. Fraedrich, and R. Voss (2001), North Atlantic decadal regimes in a coupled GCM simulation, *Clim. Dyn.*, *18*, 321–330.

Rayner, N. A., D. E. Parker, E. B. Horton, C. K. Folland, L. V. Alexander, D. P. Rowell, E. C. Kent, and A. Kaplan (2003), Global analyses of sea surface temperature, sea ice, and night marine air temperature since the late nineteenth century, *J. Geophys. Res.*, *108*(D14), 4407, doi:10.1029/2002JD002670.

Rodwell, M. J., D. P. Rowell, and C. K. Folland (1999), Oceanic forcing of the wintertime North Atlantic Oscillation and European climate, *Nature*, *398*, 320–323.

Saito, K., T. Yasunari, and J. Cohen (2004), Changes in the sub-decadal covariability between Northern Hemisphere snow cover and the general circulation of the atmosphere, *Int. J. Climatol.*, *24*, 33–44.

Slonosky, V. C., P. D. Jones, and T. D. Davies (2001), Atmospheric circulation and surface temperature in Europe from the 18th century to 1995, *Int. J. Climatol.*, *21*, 63–75.

Thompson, D. W. J., and J. M. Wallace (2000), Annular modes in the extratropical circulation. Part I: Month-to-month variability, *J. Clim.*, *13*, 1000–1016.

Torrence, C., and G. P. Compo (1998), A practical guide to wavelet analysis, *Bull. Am. Meteorol. Soc.*, *79*, 61–78.

Trenberth, K. E., and J. W. Hurrell (1994), Decadal atmosphere-ocean variations in the Pacific, *Clim. Dyn.*, *9*, 303–319.

Trenberth, K. E., and D. A. Paolino (1981), Characteristic patterns of variability of sea-level pressure in the Northern Hemisphere, *Mon. Weather Rev.*, *109*, 1169–1189.

Trigo, R. M., T. J. Osborn, and J. M. Corte-Real (2002), The North Atlantic Oscillation influence on Europe: Climate impacts and associated physical mechanisms, *Clim. Res.*, *20*, 9–17.

Walker, G. T. (1924), Correlations in seasonal variations of weather IX, *Mem. Ind. Meteorol. Dep.*, *24*, 275–332.

Wallace, J. M. (2000), North Atlantic Oscillation/annular mode: Two paradigms–one phenomenon, *Q. J. R. Meteorol. Soc.*, *126*, 791–805.

Wallace, J. M., and D. W. J. Thompson (2002), The Pacific center of action of the Northern Hemisphere annular mode: Real or artifact?, *J. Clim.*, *15*, 1987–1991.

Walter, K., and H.-F. Graf (2002), On the changing nature of the regional connection between the North Atlantic Oscillation and sea surface temperature, *J. Geophys. Res.*, *107*(D17), 4338, doi:10.1029/2001JD000850.

Yan, Z. W., M. N. Tsimplis, and D. Woolf (2004), Analysis of the relationship between the North Atlantic oscillation and sea-level changes in northwest Europe, *Int. J. Climatol.*, *24*, 743–758.

R. J. Allan and T. J. Ansell, Hadley Centre for Climate Prediction and Research, Met Office, Bracknell RG12 2SY, UK.

M. R. Haylock and P. D. Jones, Climatic Research Unit, School of Environmental Sciences, University of East Anglia, Norwich NR4 7TJ, UK. (m.haylock@uea.ac.uk)